ORNL/TM-2018/1007

A Critical Literature Review of Defrost Technologies for Heat Pumps and Refrigeration Systems

Kashif Nawaz
Ahmed Elatar
Brian Fricke

**Approved for public release.
Distribution is unlimited**

March 31, 2018

OAK RIDGE NATIONAL LABORATORY
MANAGED BY UT-BATTELLE FOR THE US DEPARTMENT OF ENERGY

ORNL/TM-2018/1007

Energy and Transportation Sciences Division

A CRITICAL LITERATURE REVIEW OF DEFROST TECHNOLOGIES FOR HEAT PUMPS AND REFRIGERATION SYSTEMS

Authors:

Kashif Nawaz
Brian Fricke
Ahmed Elatar

Date Published: 12-31-2017

Prepared by
OAK RIDGE NATIONAL LABORATORY
Oak Ridge, TN 37831-6283
managed by
UT-BATTELLE, LLC
for the
US DEPARTMENT OF ENERGY
under contract DE-AC05-00OR22725

CONTENTS

CONTENTS iii
LIST OF FIGURES v
LIST OF TABLES v
ACRONYMS vi
EXECUTIVE SUMMARY vii
ABSTRACT 1
1. INTRODUCTION 1
2. Frost GROWTH MITIGATION Measures 2
  2.1 Upstream Air Treatment 2
    2.1.1 Reducing inlet air humidity 2
    2.1.2 Preheating inlet air 3
    2.1.3 Increasing inlet airflow rate 4
  2.2 Heat Exchanger Modifications 5
    2.2.1 Adjusting fin and tube geometry 5
    2.2.2 Fin type selection 6
    2.2.3 Coating treatment on fin surface 7
  2.3 System Modification 8
    2.3.1 Vapor-injection technique 9
    2.3.2 Two-stage technique 9
    2.3.3 Adding outside heating source 9
    2.3.4 Adjusting refrigerant distribution 9
3. DEFROST Measures 11
  3.1 DEFROST BY CYCLE INTERRUPTION 11
    3.1.1 Compressor Shutdown Defrost 11
    3.1.2 Electric Heating Defrost 12
    3.1.3 Hot gas bypass defrosting (HGBD) 13
    3.1.4 Reverse cycle defrosting (RCD) 14
  3.2 EXTERNAL SOURCE BASED DEFROST 15
    3.2.1 Hot water spraying defrosting (HWSD) 15
    3.2.2 Air jet defrosting 16
    3.2.3 Ultrasonic defrosting 16
    3.2.4 Radiation based defrost 16
4. Defrost Control Strategies 17
  4.1 Time-temperature controlled defrost 17
  4.2 Time-pressure control 18
  4.3 Temperature measurement 18
  4.4 Air flow measurement 19
  4.5 Humidity measurement 19
  4.6 Refrigerant flow rate 19
  4.7 Comparison of air-side and refrigerant-side heat transfer rate 20
  4.8 Thermal insulation effect 20
  4.9 Optical sensors 21
  4.10 Artificial intelligence 23
  4.11 Miscellaneous processes 24
5. CONCLUSIONS 25
REFERENCES 25

LIST OF FIGURES

Fig. 1: Effect of frost accumulation and air velocity on air pressure drop across an evaporator coil (Stoecker 1998)....3
Fig. 2: Psychometric chart showing the processes in the exhaust and supply air streams in heat exchangers....4
Fig. 3: Psychometric chart showing the processes in the exhaust and supply air streams in energy exchangers....4
Fig. 4: Visualization of the fin surfaces before (a) and after (b) the frost formation process....4
Fig. 5: Frost behavior according to the types of louvered fin used on the front side of the evaporator: (a) equal louver pitch, (b) Type 1, and (c) Type 2 designs....6
Fig. 6: Structures of three heat exchanger types....6
Fig. 7: Comparison of frost growth on the coated (left, thickness = 0.3 mm) and the uncoated (right) surfaces....7
Fig. 8: Frost melting on the surface with parallel grooves after frosting for 30 min (T_w = 16°C, T_{in} = 2°C, RH = 75%, u = 1.16 m/s....8
Fig. 9: Images of the frosting process....10
Fig. 10: Schematic of compressor shutdown defrost....12
Fig. 11:Schematic of electric heat defrost (RCD)....13
Fig. 12: Schematic of hot gas bypass (HGB) defrost....14
Fig. 13: Schematic of reverse cycle defrosting (RCD)....15
Fig. 14: Side view of frost formation comparison (50X magnification)....17
Fig. 15: Commercially available optical sensor (New Avionics Corporation)....22

LIST OF TABLES

Table 1: Frost mitigation methods....10
Table 2: Various defrosting methods....15

ACRONYMS

ASHP	Air Source Heat Pump
COP	Coefficient of Performance
DB	Dry Bulb
DS	Degree of Super-heat
EPRI	Electric Power Research Institute
FEV	Frost Evenness Value
FPI	Fin Per Inch
HGBD	Hot Gad Bypass Defrost
LED	Light Emitting Diodes
MLP	Multi Layered Perceptron
RCD	Reverse Cycle Defrost
RH	Relative Humidity
RTTC	Refrigeration and Thermal Test Center
WB	Wet Bulb

EXECUTIVE SUMMARY

When the operating conditions are extremely cold and humid and the surface temperature of the heat exchanger well below the freezing point (lower than the dew point temperature of the air) moisture from the air stream will freeze on the surface after condensation and the frost will start growing. The frost growth degrades the performance of the system considerably. It hinders the airflow and increases the pressure drop through the coil which means more fan power is requires for to maintain the desired flow rate. With reduced flow rate due to the increase of pressure drop, system's capacity drops rapidly. In the case of heat pump the capacity of the evaporator decreases due to the airflow drop, which reduces the overall heating capacity and coefficient of performance of the heat pump. Additionally, the frost layer increases the thermal resistance to the heat transfer between the air and refrigerant. The reduction in airflow and increased thermal resistance reduces the heat energy extracted by the evaporator and decreases the heat pump capacity and efficiency. Similar process is observed for the cooling coils of commercial refrigeration system where the frost growth can dramatically reduce the system capacity. Once the performance reaches its minimum acceptable stage, a defrost process is introduced to remove the frost layer and to achieve the performance at the start of the cycle. The frost defrost process is repeated continuously. Overall the frost growth is highly undesired phenomena which can cause considerable reduction in performance of the system. This report overviews different procedures to counteract the frost growth.

- i- Various frost mitigation procedures have been reviewed and compared to access their feasibility. The methods such as air treatment before entering the heat exchanger are used to effectively eliminate or at least minimize the frost growth rate. Such procedures are discussed under two major categories, air treatment processes to mitigate the frost and appropriate system modification to minimize or eliminate the frost growth.
- ii- Regardless of the frost mitigation procedures, the frost growth is unavoidable under most of the conditions. This requires the development of effective defrost processes. Such procedures have been discussed in two major categories, the system interruption processes and frost removal through external means
- iii- Defrost control is critical to minimize the impact of process on the system efficiency. Various techniques for defrost process control have been discussed highlighting the critical aspects such as scalability and implementation.

ABSTRACT

Frost growth on heat exchanger surface is an unavoidable process which degrades the performance of heat pumps and refrigeration systems. This study provides a critical overview of the frost mitigation and defrost technology highlighting the major developments in this regard. Various air treatment procedures and system modification approaches are discussed to effectively mitigate the frost growth. Then defrost procedures based on operation interruption and external defrost sources are discussed. Finally, the control strategies for defrost processes are discussed in terms of their implementation issues and performance. The overall objective is to investigate the major developments to minimize the impact of frost growth on system performance and sustainability of the operation.

1. INTRODUCTION

Air source heat pump (ASHP) units have found applications worldwide due to their advantages of high efficiency, environmental protection, low cost and easily modification (Madani, 2015; Nishimura, 2002). Studies on ASHPs has become a critical research and development subject mainly due to improved energy efficiency compared to conventional technologies. However, when an ASHP unit operates for space heating and the ambient air temperature extremely low (-7 to 5^{o}C) and the relative humidity is relative high (greater than 65%), frost will form and accumulate on the outdoor coil of the ASHP, which becomes a major obstacle to achieving sustained performance. Over time, the frost accumulation on the coil becomes sufficient to both impede heat transfer and to dramatically increase the air-pressure drop, leading to a decrease in system performance (EHPA, 2015). To counter the effect, a defrost process is mandatory to remove the frost from the surface. Similarly, retail food stores and supermarkets operate their refrigeration systems continuously to maintain proper food storage conditions within their refrigerated display cases and storage areas. For obvious reasons, moist air becomes entrained within the refrigerated display cases and storage areas. Since the temperatures of the evaporators within the display cases and storage areas are well below the freezing temperature (lower than the dew point of the entrained air), water vapor within the air will condense and freeze on the evaporator surfaces, forming frost (Lawrence and Evans 2008). Thus, in order to maintain system performance and proper storage temperatures within the display cases and storage areas, evaporators require periodic heating to melt and remove the frost (Tassou, Datta and Marriott 2001).

Defrosting of outdoor coils for heat pumps and the display case evaporators for refrigeration systems can be achieved by several methods. Often times, the operation is stopped, and the frost then melts naturally as the evaporator fans blow air over the evaporator surfaces. To facilitate faster defrost, electrical resistance heaters are commonly deployed to heat the evaporator surfaces. In another defrost technique known as hot gas defrost, high temperature refrigerant vapor from the compressor discharge is routed through the frosted coil via a series of valves and piping. The high temperature vapor provides the required heating to melt the frost which has accumulated on the evaporator coils. Defrosting of supermarket display case evaporators is commonly controlled by a preset time cycle. Defrosts are typically scheduled to occur every six or eight hours, with a duration of 20 to 30 minutes. This method has the advantage of simplicity, reliability and low cost. However, a time-based defrosting strategy is determined from worst case conditions to ensure complete defrosting under extreme conditions. Thus, unnecessary defrost cycles will likely occur, thereby reducing the energy efficiency of the refrigeration system (Tassou, Datta and Marriott 2001). A significant amount of energy is required to defrost the evaporators in refrigerated display cases. Mei et al. (2002) report that electric defrost heaters can account for up to 25% of the total electrical energy consumption of refrigerated display cases. A review of manufacturers' data indicates that electric defrost energy consumption can range from 10% to 30% of the total display case energy consumption, with an average of approximately 20% (Hussmann 2011). Furthermore, defrosting adds heat to the refrigerated display cases, which must be removed by the refrigeration system after termination of the defrost cycle, thereby increasing compressor operation and energy use.

2. FROST GROWTH MITIGATION MEASURES

Frosting duration accounts more than 80% of operation time in a frosting-defrosting cycle, and thus exploration of frost retarding measures plays an important role in designing ASHP and commercial refrigeration units. To improve their operating performance, frost retarding measures attract more and more attention. Previous studies on developing frost retarding measures are broadly classified into three major types: upstream treatment of air, coil design adjustments and system adjustment.

2.1 UPSTREAM AIR TREATMENT

Frost formation and growth on the cold surface is depends on the ambient air conditions. Parameters such air temperature, RH, and airflow rate directly impact the frost density, growth rate on the heat exchanger surface. Following section briefly describes the various parameters which can influence the frost growth rate and proposes techniques which can potentially considerably reduce the phenomena.

2.1.1 Reducing inlet air humidity

Since frost forms due to solidification of water vapors, any measures of reducing inlet air humidity (such as using solid/liquid desiccants) can assist to mitigate the frost growth. Such techniques seem more applicable for a closed environment (display cases for a refrigeration system) rather for an open environment (outdoor coil of an ASHP) (Tassou et al., 2001; Yao e al., 2004). Several investigators have evaluated procedures to dehumidify the air-stream and methods such as applications of desiccants have been implemented. Wang et al. (2005) proposed the deployment of an adsorbent bed to dehumidify the air to effectively reduce the frost formation on heat exchangers. Wang et al. (2015) conducted an experimental study for a novel heat pump water heater and observed that the evaporator remained frost-free for 32, 34, 36 min during heating mode at the ambient temperatures of -3°C, 0°C and 3°C, respectively, for 85% RH. Su and Zhang (2017) evaluated the performance of a novel frost-free ASHP system combined with membrane-based liquid desiccant dehumidification. In another study, Jiang et al. (2014) introduced a novel non-frosting ASHP system, in which a glycerol solution spray system was employed to the outdoor heat exchanger to avoid frosting. The ambient relative humidity greatly affects the amount of frost formation (Tassou, Datta and Marriott 2001). Thus, relative humidity is directly related to the required defrosting frequency and associated energy use. Several studies have reported on the energy use associated with defrost heaters as a function of relative humidity (Tassou and Datta 1999) (Henderson and Khattar 1999) (Kosar and Dumitrescu 2005). Other factors which influence the rate of frost formation on evaporator coils include ambient air temperature, heat exchanger's fin spacing, and air flow rate (Bullard and Chandrasekharan 2004). Fig. 1 shows the relationship between frost accumulation, air velocity and air pressure drop across an evaporator coil (Stoecker 1998). The data shown in Fig. 1 is for a heat exchanger with a fin spacing of 4 fins per inch (1.6 fins per cm) and entering air conditions of 32°F (0°C) and 72% relative humidity. It can be seen that the pressure drop across the heat exchanger increases with increasing frost accumulation and with increasing air velocity. As frost accumulates, the size of the air passages through the coil are reduced, resulting in an increase in the pressure drop through the coil and an increase in the air velocity through coil. Thus, it has been suggested that defrost initiation can be based either on the increase in pressure drop across the evaporator or on the increase in air velocity through the evaporator, both of which accompany an increase in frost accumulation.

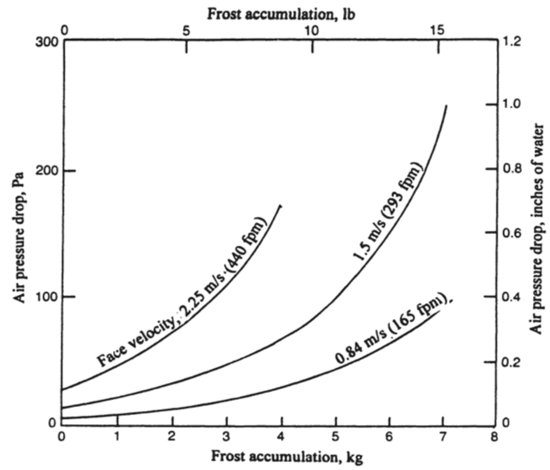

Fig. 1: Effect of frost accumulation and air velocity on air pressure drop across an evaporator coil (Stoecker 1998)

Regardless of the potential benefits of the above described processes, it important to account for the increase in capital and operational costs. Additionally, the desiccant regeneration process requires energy, and thus, makes the process more energy intensive. However, since during the dehumidification process, air temperature is increased due to the heat of adsorption, the process provides a secondary benefit which helps to minimize the frost growth as described in the following section.

2.1.2 Preheating inlet air

Another obvious choice to mitigate the frost is preheating inlet air which is a simple and effective technique. However, it is not easy to implement and requires high energy, particularly in relatively cold regions. Using waste heat in preheating inlet air is a feasible option where for example, heat recovered from exhausted indoor air, can be effectively utilized. Conventionally heating elements are placed in the inlet air duct so that when outdoor air temperature drops below the frosting point, the heating elements can preheat the air to avoid frost growth. Rafati et al. (2014) reported that to prevent frost formation, the inlet air temperature upstream of an outdoor coil must always be higher than the frosting point.

Figure 2 and 3 present the frost formation conditions for a heat exchanger and for an energy exchanger. Kwak and Bai (2010) conducted an experimental study to increase the heating capacity and COP of a small capacity heat pump using the air as a heat source under frosting conditions, deploying an electric heater at the entrance of outdoor unit of heat pump. They concluded that when the outdoor temperature was 2°C/1°C (DB/WB), the heating capacity and COP were increased by 38.0% and 57.0%, respectively, compared to the performance of a conventional heat pump.

Several studies have focused on the heat recovery process as a frost retarding measure (Rafati et al., 2014; Kragh et al., 2005). The process relies on the heat transfer between the exhausted indoor air and ambient air to reduce the frost growth rate. Song (2014) compared different frost mitigation measures and showed that preheating inlet air is not feasible in regions with long periods of very low outdoor air temperatures, from −54 to 10°C. Thus, for such situations the source for preheating inlet air should be waste heat, such as heat recovered from exhausted indoor air or waste water.

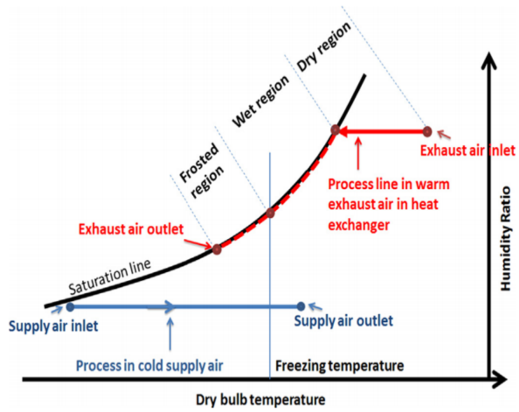

Fig. 2: Psychometric chart showing the processes in the exhaust and supply air streams in heat exchangers

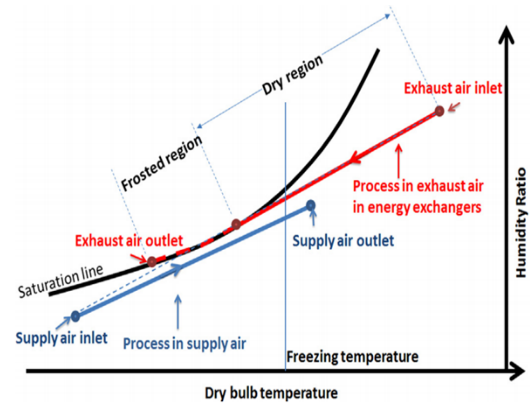

Fig. 3: Psychometric chart showing the processes in the exhaust and supply air streams in energy exchangers

2.1.3 Increasing inlet airflow rate

Increasing inlet airflow rate is another potential technique to minimize the frost growth, but this results in increased fan power and noise level, both of which are major disadvantages. Da Silva et al. (2011) conducted an experimental study to investigate the effect of frost accumulation on the thermo-hydraulic performance of tube-fin evaporator coils. They observed that the frost accumulation rate increased with the air flow rate, supercooling value and fin density. They concluded that airflow rate reduction was a dominant factor for the drop in the capacity of evaporator. To predict the performance of an outdoor coil considering airflow reduction due to frost growth, a numerical model was developed and validated by Ye and Lee (2013). They concluded that convective thermal resistance between the frost surface and air results in 90% of the total thermal resistance; the conductive thermal resistance from the tube wall to the frost surface is only 2–5% of the total resistance. In addition, the increase in the convective thermal resistance from the air to the frost surface varies the most as a function of the blockage ratio due to the growth of the frost layer. Moallem et al. (2013) studied the frost formation on louvered folded fins in outdoor microchannel heat exchangers used in air source heat pump systems. They found that for louver fin variation of the fin width did not improve the frosting performance of the fins significantly, but increasing the fin depth seemed to increase the fin capacity (39%) with some penalization of the frosting time (6%). Additionally, increasing air velocity from 0.8 m/s (157 fpm) to 1.6 m/s (315 fpm) improved the capacity of the fins up to 53%.

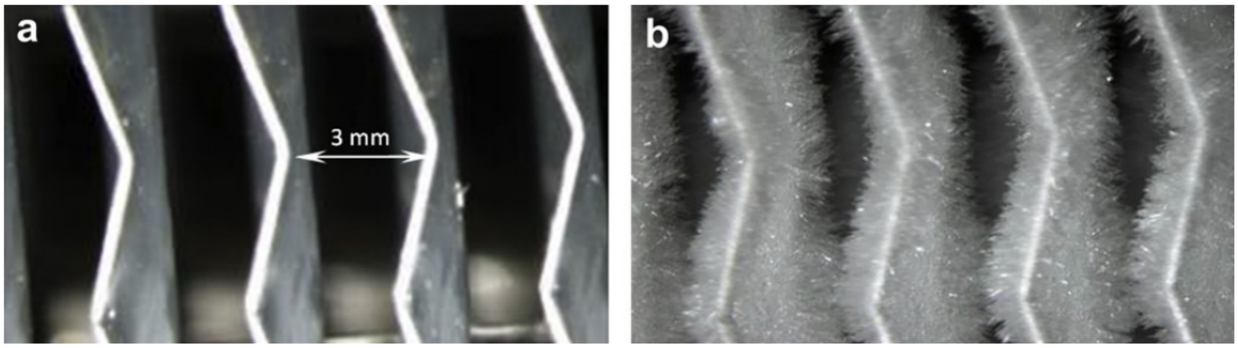

Fig. 4: Visualization of the fin surfaces before (a) and after (b) the frost formation process

2.2 HEAT EXCHANGER MODIFICATIONS

Passive procedures rely on the modification of the equipment to reduce the frost growth on the heat exchanger surface. Such methods include adjusting the fin design, coil circuiting and system design.

2.2.1 Adjusting fin and tube geometry

Fin density, often measured in fins per inch (FPI), is a critical parameter for heat exchanger design. Due to the requirements of compact design and reduction in manufacturing cost, there has been a trend of increasing the fin density which has led to a reduction in space between two adjacent fins. Yang (2003) conducted a detailed study to investigate the effects of the staging fin on the frost/defrost performance of heat pump outdoor coils under different operating conditions. A series of frosting tests was conducted on an off-the-shelf heat pump system with five (three two-row and two three-row) evaporators over a range of outdoor temperatures and relative humidity and a range of airflow rates typical of those found in residential sized heat pumps. Yan et al. (2003) reported that the rate of pressure drop increases rapidly as the relative humidity increases when a heat exchanger is operating under frosting conditions and the performance of the heat exchanger is not impacted significantly by the fin pitch provided the fin spacing is large. Yang et al. (2006) proposed optimal values of design parameters for a fin-tube heat exchanger of a household refrigerator under frosting conditions to improve its thermal performance (5.5% increment) and to extend its operating time (12.9% improvement). Lee et al. (2010) measured and analyzed the air-side heat transfer characteristics of flat finned-tube heat exchangers at different fin pitches, numbers of tube rows and tube alignment under frosting conditions, and found that the air flow rate of the heat exchangers decreased with time because of frost growth. However, the effect of the number of tube rows on the reduction in the air flow rate was relatively smaller than that of the fin pitch. The staggered tube alignment showed more rapid air flow reduction with time than the inline tube alignment due to the higher flow restriction in the staggered tube alignment. The heat transfer rate increased with the decrease of the fin pitch and increase of the number of tube rows. Equation (1) and (2) present the Colburn j factor for inline and staggered tube arrangement.

$$j_{inline} = 0.0066 \times \mathrm{Re}_{D_h}^{0.0526} \times \left(\frac{D_h}{F_p}\right)^{0.4513} \times Fo^{-0.0210} \tag{1}$$

$$j_{staggered} = 0.0006 \times \mathrm{Re}_{D_h}^{0.3734} \times \left(\frac{D_h}{F_p}\right)^{0.2134} \times Fo^{-0.0777} \times N^{0.0545} \tag{2}$$

Park et al. (2016), recently demonstrated that the frost blocking of the spaces between louvers at the front side of an evaporator can be delayed and the thermal performance can be improved by 21% when unequal louver pitch design was used compared to the equal louver pitch case. Sommers and Jacobi (2005) investigated the performance of a vortex generator deployed on plain fin and tube heat exchangers and concluded that vortex generation exhibits reasonable tolerance to frost, incurs only a small penalty in pressure drop, and significantly reduces the air-side thermal resistance.

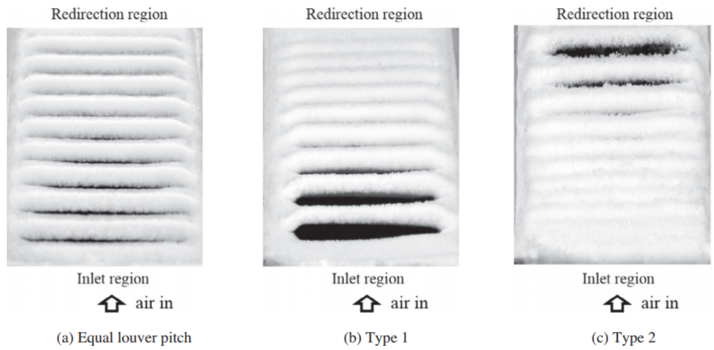

Fig. 5: Frost behavior according to the types of louvered fin used on the front side of the evaporator: (a) equal louver pitch, (b) Type 1, and (c) Type 2 designs

2.2.2 Fin type selection

Fin type can considerably impact the heat transfer and pressure drop of heat exchangers and, for obvious reasons, the heat exchanger performance is highly impacted by the type of fin design deployed. Yan et al. (2005) experimentally investigated the operating performance of frosted finned-tube heat exchangers with flat plate fins, one-sided louver fins and re-direction louver fins. For comparable conditions, the heat exchanger with re-direction louver fins performed worst compared to the other two types of heat exchangers. Huang et al. (2014) experimentally compared the effects of periodic frosting-defrosting performance by using three fin types in an outdoor coil of a residential ASHP unit. The outdoor coil with flat fins demonstrated the best thermal performance in the periodic frosting/defrosting cycles of the ASHP unit, followed by the outdoor coils with wavy and louver fins, respectively. Zhang and Hrnjak (2009) experimentally studied three types of heat exchangers with louver fin geometry under dry, wet and frost conditions. The configurations included: (1) parallel flow serpentine fins with extruded flat tubes, (2) parallel flow parallel fins with extruded flat tubes, and (3) round tube wave plate fins. Under frosting conditions, the heat exchanger with round tube wave plate fin showed the longest refrigeration time due to its largest surface area. The increase in air-side pressure drop for the parallel flow parallel fins with extruded flat tubes heat exchanger was the lowest.

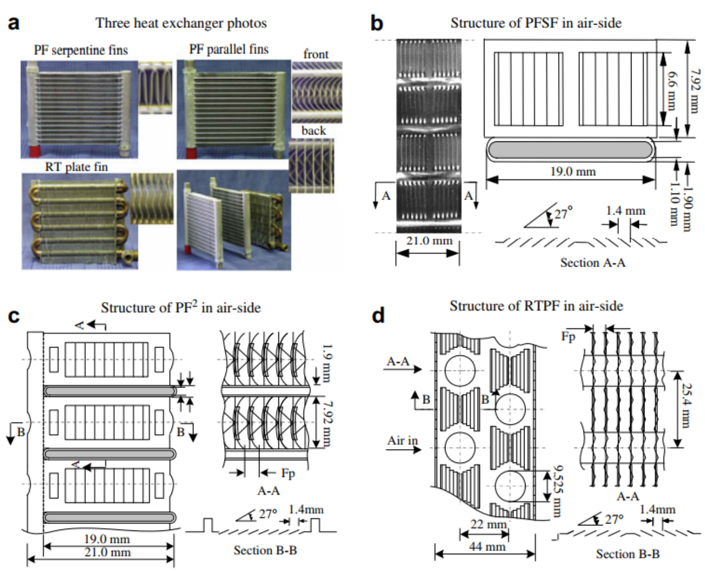

Fig. 6: Structures of three heat exchanger types

2.2.3 Coating treatment on fin surface

Frost growth rate and density highly depend on the surface characteristics. Parameters such as liquid-solid contact angle is perhaps mostly widely used to describe the surface morphology. Several researchers have investigated the impact of surface type and associated frost growth rate. Often times, the surface morphology has been modified and the influence has been evaluated. Such studies include mostly small-scale studies where a relatively small metal piece represented the fin surface. However, recently several researchers have tested full heat exchangers with modified surfaces and the appropriateness of such procedures have been discussed for ASHP and refrigeration systems.

Okoroafor and Newborough (2000) found that frost growth on cold surfaces exposed to warm humid air streams could be reduced significantly by the presence of cross linked hydrophilic polymeric coatings. The frost thickness was decreased in the range of 10–30% when compared to using an uncoated metallic surface. In another study, Wu and Webb (2001) investigated both frosting and defrosting processes on hydrophilic and hydrophobic surfaces, showing a hydrophilic coating was preferable for operation under frosting conditions. Cai et al. (2011) experimentally studied the frosting conditions on a normal copper surface, a hydrophobic coating (car wax coating) surface and a hygroscopic coating (glycerol coating) surface. Based on the distribution of ice crystals and time of frost appearance, the hygroscopic coating performed better than the hydrophobic coating; however, based on parameters such as coating thickness, thermal resistance and expansion defect of the hygroscopic coating, the hydrophobic coating was found to be superior to the hygroscopic coating.

Jhee et al. (2002) conducted an experimental study on hydrophilic and hydrophobic treated heat exchangers and reported that a relatively higher density formed on a hydrophilic surface during frosting, and the water draining rate during defrosting was higher. On the other hand, for a hydrophobic surface the frost density was lower and the draining water rate during the frost melting process was increased mainly due to large chunks of incompletely melted frost. They concluded that the hydrophilic treatment influences the behavior of frosting while the hydrophobic treatment becomes more important during defrosting.

Liu et al. (2006) deployed a novel anti-frost paint on a cold metal surface and observed that the onset of frost formation was delayed by at least 15 min. The thickness and the mass of the deposited frost layer was reduced by at least 40% compared with that on the uncoated copper surface. While evaluating the long-term performance, they found that the growth of frost crystals on the surface of the paint coating was similar to that of a hydrophobic surface. The frost growth exhibited strong dendritical characteristics, and the frost layer formed had a very loose, weak, and fragile structure that could be easily removed by external force. It is important to note that the deployment of a polymer layer introduced a thermal resistance due to its lower thermal conductivity.

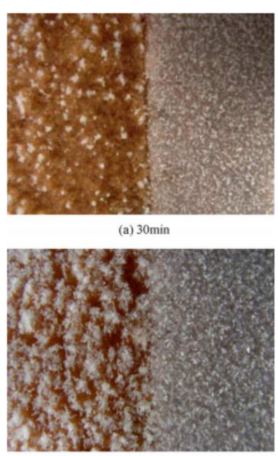

Fig. 7: Comparison of frost growth on the coated (left, thickness = 0.3 mm) and the uncoated (right) surfaces

Several researchers have investigated the influence of surface morphology at micro or nano-scale to understand the processes such as nucleation of droplets and merging of droplets which dramatically impacts the frost density and adhesion to the surface. Chen et al. (2013) reported a hierarchical surface which allows for inter droplet freezing wave propagation suppression and efficient frost removal. It was demonstrated that the enhanced performance is mainly due to the activation of the microscale edge effect in the hierarchical surface, which increases the energy barrier for ice bridging as well as engendering the liquid lubrication during the defrosting process.

Zuo (2017) prepared a superhydrophobic surface where ZnO (Zinc Oxide) nanorods were deployed through radio frequency magneton sputtering method. They found that the frost formation on the as-prepared SHP ZnO surface was effectively delayed for over 140 min even at -10°C. The superhydrophobic surface exhibited an excellent durability against repetitive frosting/defrosting. Wu (2017) conducted a study to investigate the condensation, frost crystal growth, frost melting and meltwater drainage characteristics on aluminum surfaces with parallel and crossed grooves. They found the parallel grooved surface had better drainage than the flat surface with a smaller meltwater retention ratio, while the surface with crossed grooves had worse drainage.

Sommer et al., (2016) noted that existing frost density correlations found do not include surface wettability (i.e. contact angle) as a parameter in the model. However, surface wettability is important in accurately determining the properties of the frost layer and thus should be included in future frost correlation development efforts. They evaluated the effect of surface energy on the frost thickness and density for both a hydrophobic substrate and a hydrophilic substrate and found that the frost layer on the hydrophobic surface was ''thicker and fluffier" resulting in a less dense frost than the frost on the baseline surface. Liang et al., (2015) designed a frosting/defrosting experiment to study the effects of surface characteristics on defrosting behaviors of a fin. The characteristics of frost melting and molten water retention were analyzed and compared. It was concluded that effects of the surface characteristics on the melting time and melting process were significant.

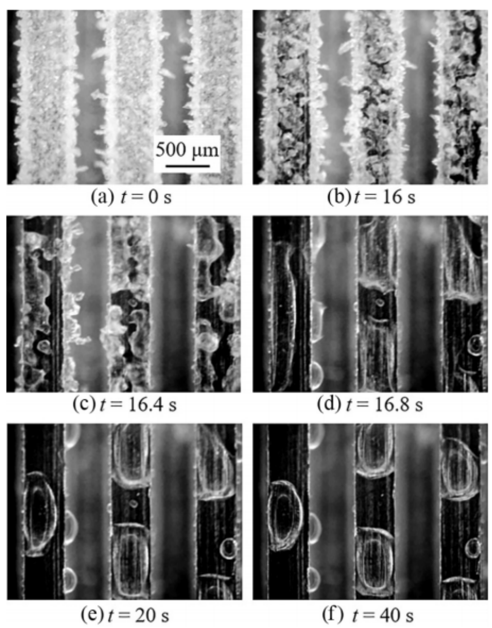

Fig. 8: Frost melting on the surface with parallel grooves after frosting for 30 min (T_w = 16°C, T_{in} = 2°C, RH = 75%, u = 1.16 m/s

2.3 SYSTEM MODIFICATION

There are also some outside of system type frost retarding measures for ASHP units, which have been undertaken through adjusting and optimizing the structure of the system. In these measures, all the energy consumed on frost retarding comes from heat transferred from the refrigerant inside the system to the tube and fins.

2.3.1 Vapor-injection technique

The vapor-injection technique has been used mainly for room air conditioner applications since the 1980s, but its applications to heat pump units received more attention recently, since the process can mitigate frosting in cold climates. Zhnder et al. (2002) conducted an experimental study for an air-water vapor-injection heat pump unit at an inlet air temperature of −7°C. They observed an increase in heat output of 28% and a COP improvement of 15%, respectively, when compared to the performance without injection. Similarly, Nguyen et al. (2007) evaluated the thermal performances of a flash tank vapor injection cycle and a sub-cooler vapor injection cycle using R407C, reporting their heating COPs 24% and 10% higher compared to a single-stage cycle, respectively. Shao et al. (2002) concluded that a vapor-injection heat pump unit could provide enough heating capacity even when the outdoor temperature is in range of −20 to −15°C. In another study, Ma and Zhao (2008) experimentally investigated the operating performance of an ASHP unit with a flash-tank coupled using scroll compressor with an ambient temperature of −25°C. They found that the ASHP unit was more efficient than the system with a sub-cooler at −25 to −7°C.

2.3.2 Two-stage technique

Similar to the vapor-injection technique, the two-stage technique can result in considerably improved performance for a heat pump. Wang et al. (2005) experimentally investigated a double-stage heat pump heating system, which coupled an ASHP unit and a water source heat pump unit. They showed that the proposed system offered an average energy efficiency ratio up to 3.2 and the average indoor temperature exceeded 19.5°C, minimum at 18°C in test period. In another study, Li et al. (2011) proposed and experimentally tested a new frost-free ASHP system, indicating the novel system could operate more efficiently than a conventional ASHP unit in winter. Heo et al. (2010) reported that that the COP and heating capacity of a two-stage vapor injection cycle were enhanced by 10% and 25%, respectively, when the ambient temperature was −15°C. Similarly, Wang et al. (2009) demonstrated that a COP improvement of 23% for a two-stage heat pump system can be achieved when the ambient temperature was −17.8°C. Bertsch and Groll (2008) tested a specially designed R410A two-stage ASHP unit with a heating COP of 2.1 at an ambient temperature of −30°C.

2.3.3 Adding outside heating source

Adding an outside heat source could improve the system operating performance under frosting conditions. Mei et al. (2002) reported that the heating capacity of an ASHP unit could be increased, and the frost accumulation on its outdoor coil can be reduced by heating up the liquid refrigerant in its accumulator. By heating liquid refrigerant, the frequency of defrosting cycles was reduced by a factor of 5 and indoor supply air temperature raised by 2 to 3°C because of the increased compressor suction pressure. It is important to distinguish that this is different from heating the inlet air of the outdoor coil (discussed in Section 2.1.2) since the heat is add directly to the refrigerant loop. Regardless, both processes are energy intensive and to improve the economy of the ASHP units. The heating source should be waste heat, such as heat recovered from exhausted indoor air or waste water. This type of frost retarding measure is limited in application, due to its disadvantages of high operating cost and additional infrastructure.

2.3.4 Adjusting refrigerant distribution

For an outdoor coil used in an ASHP unit, multiple refrigerant circuits are deployed to minimize the refrigerant pressure drop and to achieve an enhanced heat transfer rate. Interestingly, the frost accumulation is mostly uneven on the surface of a multi-circuit heat exchanger, a phenomenon known as mal-defrost.

Wang et al., (2012) conducted a field test to quantify the performance drop of an air source heat pump (ASHP) system under a special kind of mal-defrost phenomenon appearing in moderate climate conditions. The mal-defrost was found with the more than 60% frosted area of the outdoor heat exchanger after the system running 5 days. Comparing the test data before and after frosting, it was found that the mal-defrost decreased the COP up to 40.4% and the heating capacity to 43.4%. Qu et al., (2012) conducted an experimental study to analyze the reverse cycle defrost performance for a four-circuit outdoor coil in an ASHP unit. It was observed that defrosting was quicker on the airside of upper circuits than that on the lower circuits. The effects of downward flowing melted frost along a multi-circuit outdoor coil surface had a significant impact on overall performance and the defrosting efficiency of 34.5% was reported for system.

In another study Song et al., (2016a,2016b) reported that when a vertically installed multi-circuit outdoor coil in an ASHP unit was changed to a horizontally installed coil, the defrosting efficiency increased from 43.5% to 53.3%, or an increase of 9.8%. Additionally, the negative effects of melted frost flowing downward due to gravity were eliminated. They defined the parameter frosting evenness value (FEV) as the ratio of the minimum frost accumulation among three circuits to the maximum value. In another study to investigate the relationship of FEV and frost retarding effect, Song et al., (2016c) found that as FEV increased from 75.7% to 90.5%, the average COP was increased from 4.10 to 4.26 for a 3600 s frosting process, and increased from 3.18 to 4.00 during the last 600 s.

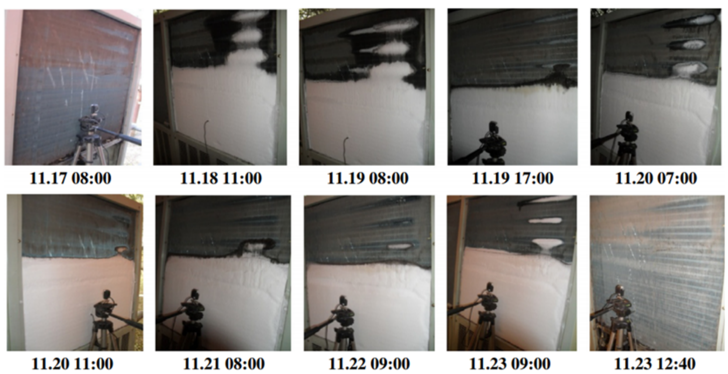

Fig. 9: Images of the frosting process

In Table 1, a relative comparison of various frost mitigation processes is provided. It is important to note that nearly all the measures would increase the initial cost and/or the operational cost. System adjustment would increase the system complexity and decrease system stability. Additional thermal energy is required for the measures of preheating inlet air and adding an outside heat source. Among all the measures, reducing inlet air humidity and preheating inlet air have the best frost mitigation effect. Considering the comprehensive values of listed measures, preheating inlet air with waste heat and coating treatment on fin surface with new materials are highly recommended for further study.

Table 1: Frost mitigation methods

Method	System complexity	System stability	Frost Mitigation	Scalability	Increase in capital cost	Increase in operational cost
Reducing air humidity	High	High	High	Moderate	High	High
Preheating the air stream	High	High	High	Moderate	High	High
Increasing air flow rate	High	High	Moderate	Moderate	High	High
adjusting fin geometry	Low	High	Moderate	High	Moderate	Low
Fin type selection	Low	High	Low	High	Moderate	Low
Surface morphology for fin surface	Moderate	High	Moderate	Moderate	Moderate	Low
Vapor injection technique	High	Low	Moderate	Low	High	Moderate

Method	System complexity	System stability	Frost Mitigation	Scalability	Increase in capital cost	Increase in operational cost
Two stage technique	High	Low	Moderate	Low	High	Moderate
Adding outside heat source	Moderate	Moderate	Moderate	Moderate	Moderate	High
Adjusting refrigerant distribution	Low	High	Moderate	Moderate	High	Low

3. DEFROST MEASURES

As discussed earlier, the presence of frost on tube surface of the outdoor coil in an ASHP unit would deteriorate its operating performance, energy efficiency, reliability and life span. While the use of frost mitigation measures can delay frost formation or growth, these measures are often expensive to implement and operate. Even in their presence, frost accumulation is unavoidable. Therefore, appropriate defrosting measures are critical to achieve the satisfactory operation of the equipment. It is important to understand the relative difference between frost mitigation and defrost procedures. While frost mitigation processes aim at suppressing the frost growth, the defrost process is mainly focused on removing the frost layer which has been developed. Another important difference is the type of operation. Most frost mitigation procedures are continuous processes while the defrost process can be intermittent.

This section provides a brief description of various defrosting methods. Based on type of operation the defrosting techniques can be broadly divided into two major types: (1) Defrost by cycle interruption, and (2) Defrost by external factors. The first type of defrosting includes procedures such as compressor shutdown defrosting, electric heating defrosting, hot gas bypass defrosting, and reverse cycle defrosting. The second type of defrosting includes advanced procedures such as hot water spraying defrost, gas jet defrost, ultrasonic defrost and radiation based defrost.

3.1 DEFROST BY CYCLE INTERRUPTION

3.1.1 Compressor Shutdown Defrost

The most basic defrost method is the off-cycle defrost, in which the refrigerant flow to the evaporator is interrupted. The evaporator fans then blow air across the frosted evaporator, thereby melting the accumulated frost. Since this method relies on the circulation of relatively warm air over the evaporator to melt the frost, this technique is limited to where ambient air temperature is not lower than 1ºC. When defrosting is needed, as shown in Fig. 10, the compressor is shutdown however the outdoor coil air fan continues to move the ambient air to pass through the outdoor coil to melt the frost.

The effectiveness of compressor shutdown defrosting method was demonstrated by Shang (2009), by experimentally investigating the effect of pre-start fans on defrosting performance of an ASHP unit. The low initial cost, avoidance of complicated process and easy to control make this process widely adoptable. However, since the energy for defrost comes from ambient air, this defrosting method requires substantially longer duration for complete removal of frost.

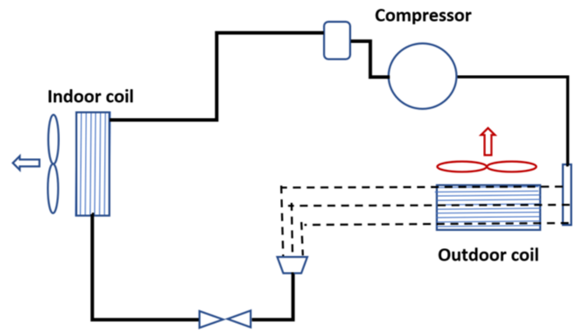

Fig. 10: Schematic of compressor shutdown defrost

3.1.2 Electric Heating Defrost

Electric defrost methods make use of electrical heating elements which are mounted adjacent to the evaporator coil or integrated into the evaporator coil. During a defrost cycle, the refrigerant flow to the evaporator is interrupted and the heating elements are energized. The evaporator fans then blow hot air over the evaporator surface. Radiation, conduction and/or convection heat transfer between the heating elements, air and the evaporator cause the frost to melt. Electric heating defrosting usually involves electrically heating up the surface of an outdoor coil to melt off frost. Since heat is being added externally to the evaporator, only a portion of the heat generated is used to melt the frost. The remaining portion of the heat is transferred to the surroundings. Approximately 1% or more of the heat generated by the electric defrost heaters goes into melting the frost while the remaining excess heat is transferred to the air and food products within the display case. This excess heat must then be removed when the refrigeration system resumes operation after the defrost cycle. Compared to off-cycle defrosting, the electric defrost method is relatively quick. In addition, electric defrost has low first cost but high operating cost. Bansal et al. (2010) conducted a thermal analysis of a defrost cycle in order to design more efficient defrosting mechanisms in household refrigerators and freezers. They developed heat transfer model to determine energy flows from a defrost heater across various components of a refrigerator/freezer and reported that a radiant defrost heater was not the best option to use. The temperatures that the radiant heater reaches were described as unnecessarily high for the purpose of melting the frost on the evaporator. In another similar study Melo et al., (2013) evaluated the performance of defrost systems applied to household refrigerators. Three distinct types of electrical heaters (distributed, calrod and glass tube) and three actuation modes (integral power, power steps and pulsating power) were investigated. It was found that the defrost efficiency of the three types of heaters is practically the same for each operating mode. The highest efficiency of approximately 48% was obtained with the glass tube heater operating in power steps.

Experimental study was carried out to investigate feasibility and efficiency of the defrost method with air bypass circulation and electric heater for cold storage. Five defrost cases with different defrost heaters and defrost air circulation modes were comparatively studied. The conclusions are as following (1) During defrosting, circulating air was helpful to improve the defrost speed, but it easily leaded to a large fluctuation of the storage temperature. With the same input power, heater embedded in fins was more effective than the one installed in front of evaporator. Case Ⅴ was the optimum implementation way of the novel defrosting method. Yin et al. (2012) investigated a a novel defrost method with air bypass circulation and electric heater. Five case studies of this new method with different defrost heaters and air circulation modes were comparatively studied. The results showed that the case with heater embedded in evaporator fins and air circulating through bypass channel was the optimum and compared to the traditional heater defrost method, the defrost time and defrost energy consumption of this new method was reduced by 62.1%, and 61.0% respectively.

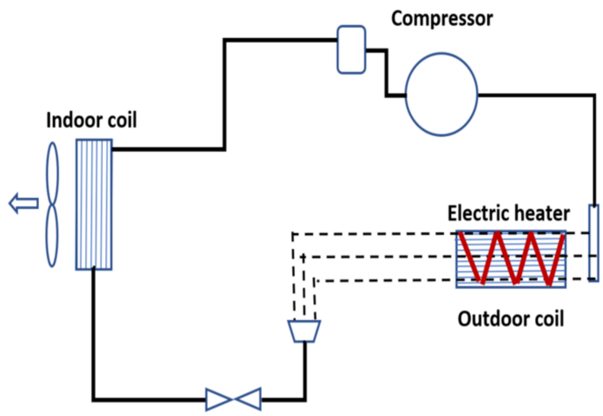

Fig. 11:Schematic of electric heat defrost (RCD)

3.1.3 Hot gas bypass defrosting (HGBD)

Hot gas bypass defrosting generally applied to commercial ASHP units. As shown in Fig. 12, the superheated refrigerant vapor discharged from compressor is directed into an evaporator, or outdoor coil, bypassing a condenser and an expansion device which allows high pressure, high temperature refrigerant gas from the compressor discharge to flow into the frosted coil. As the hot refrigerant gas flows through the coil, it condenses, thus releasing its latent heat. This warms the heat exchanger and melts the frost (Hoffenbecker, Klein and Reindl 2005).

Choi et al., (2011) reported that hot gas bypass defrost method was 13% better than the Reverse Cycle Defrost (RCD) cycle. Furthermore, the recovery time of the RCD method was three times longer than that of the HGBD method since the evaporator temperature using the RCD method was found to be higher than that of the HGBD method. Jang et al., (2013) designed a dual hot gas spray defrosting method and compared defrost performance to traditional reverse cycle defrosting method. They found that the total heating capacity was increased by 17% and the input power was increased by 7.8%. Finally, the total energy efficiency was increased by 8% compared to reverse cycle defrosting. Compared to electric defrosting, hot gas defrosting can remove the accumulated frost approximately 1.5 times faster (Rainwater 2009). In addition, since the evaporator is being heated from the inside, the amount of excess heat transferred to the display case and food products is less than that associated with electric defrost. It has been estimated that only 15% to 25% of the heat generated by hot gas defrost goes into melting the frost while the remaining excess heat is transferred to the surroundings (Niederer 1976).

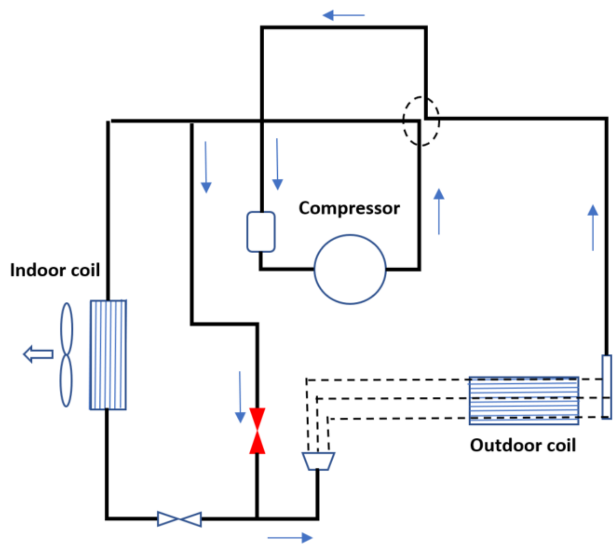

Fig. 12: Schematic of hot gas bypass (HGB) defrost

3.1.4 Reverse cycle defrosting (RCD)

When an ASHP unit is operated at reverse cycle defrosting mode, its outdoor coil acts as a condenser and its indoor coil as an evaporator. During defrosting, hot gas is pumped into an outdoor coil to melt off the frost. When the frost is melted and drained away from the coil, the ASHP unit returns to heating operation. It is important to note that besides a four-way valve, reverse cycle defrosting does not require any complicated components. That means the system is simple and easily to install. The energy used for reverse cycle defrosting mainly comes from four sources: (1) thermal energy of indoor air, (2) Stored energy of indoor coil, (3) electricity input to indoor air fan, and (4) electricity input to compressor. The energy is consumed in five aspects, (1) heating outdoor coil metal, (2) latent heat melting frost, (3) Sensible heating of the melted frost, (4) vaporizing retained water, and (5) heating ambient air. The duration of a reverse cycle defrosting operation much shorter than that of hot gas bypass defrosting. In fact, reverse cycle defrosting has been the most widely used as a standard defrosting method for ASHP units for many years.

Dong et al., (2012) conducted an experimental study on defrosting energy supplies and consumptions during a revere cycle defrost operation for an experimental ASHP unit. The experimental results indicated that the heat supply from indoor air contributed to 71.8% of the total heat supplied for defrosting and 59.4% of the supplied energy was used for melting frost. The maximum defrosting efficiency could be up to 60.1%. However, taking heat away from indoor air in a heated space can adversely affect indoor thermal environment and indoor thermal comfort level. Qu et al., (2012) reported that the performance of a reverse cycle defrost operation for an ASHP unit an electronic expansion valve using two different control strategies: fully open and controlled by a DS (Degree of superheat) controller. Experimental results suggested that when the EEV was regulated by a DS controller during defrosting, a higher defrosting efficiency obtained. The refrigerant flow rate was decreased during the latter part of a defrosting operation and thus less heat was generated, consequently a higher defrosting efficiency and less heat wastage was observed.

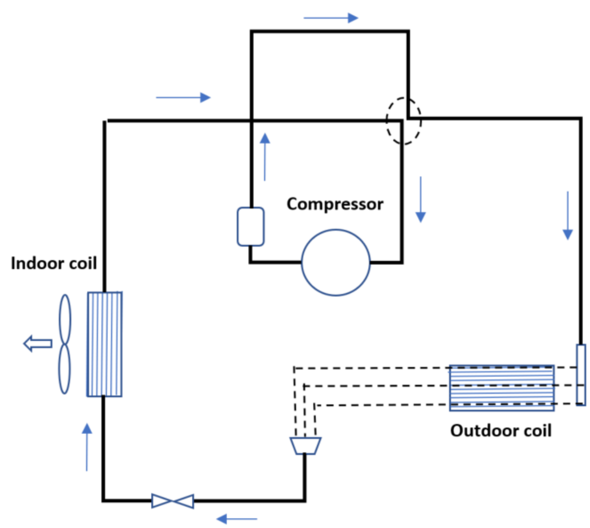

Fig. 13: Schematic of reverse cycle defrosting (RCD)

To clearly distinguish the various defrosting methods discussed under this section, their operation differences and evaluation results are summarized in Table 2. To decrease the defrosting duration, only reverse cycle defrosting needs turning on the indoor air fan, and compressor shutdown defrosting would turn on the outdoor air fan. For hot gas bypass defrosting and reverse cycle defrosting, the compressor should be turned on to supply enough defrosting energy. Hot gas bypass defrosting has good system stability and defrosting effect; however, more electric energy is needed than that consumed by reverse cycle defrosting.

Table 2: Various defrosting methods

Method	ID fan	OD fan	Compressor	Thermal source	System complexity	System stability	Defrost effect	Scalability	Efficiency degradation
Compressor shutdown	Off	ON	OFF	Ambient air	Low	High	Low	High	Moderate
Electric heater	Off	OFF	OFF	Electric power	High	High	High	Moderate	High
Hot gas bypass	Off	OFF	ON	Electric power	Moderate	Moderate	Moderate	Low	Moderate
Reverse cycle	ON	OFF	ON	Electric power	High	Low	High	Low	High

3.2 EXTERNAL SOURCE BASED DEFROST

3.2.1 Hot water spraying defrosting

Under this method the frost is be melted using a hot water spray on the frosted coil. This is a relatively new method and only limited reported studies can be identified including. Abdel-Wahed (1983) experimentally investigated applying hot water spraying defrosting method to a horizontal flat plate surface. They found that the variation of the frost layer with time is approximately linear. Hot water source is one important limitation for application. In addition, at the termination of hot water spraying defrosting, there would be some water retained on the surface of fin due to surface tension. The retained water would degrade system operating performance when it changes to heating mode.

3.2.2 Air jet defrosting

Air jet defrosting techniques use the kinetic energy of air to detach the frost from the heat exchanger surface. Fukiba et al., (2009) conducted a study to defrost a heat exchanger where the air jet impinged on the heat exchanger surface for a short duration (e.g., 0.1 s) at intervals of 10–50 s. This study revealed that this method was successful when the velocity of the main airflow was low and the temperature of the cooling tubes was cryogenic. However, all frost could not be removed under other conditions in which the frost was strongly attached to the cooling tubes. To improve the procedure, Sonobe et al., (2015) developed a new method for defrosting cooling tubes in heat exchangers in which frost is removed using solid particles and an air jet. They reported that the proposed defrosting method was more effective than a previous method that uses only an air jet.

3.2.3 Ultrasonic defrosting

The ultrasonic defrosting technique relies on vibrational energy to detach and remove the frost from the coil surface. The main mechanism of ultrasonic frost suppression has been attributed to the high frequency ultrasonic mechanical vibrations that can break up frost crystals and frost layers, then frost will fall off with the gravity. Li et al., (2010) conducted an experimental study of frost formation on a cold flat surface to analyze the impact of 20 kHz ultrasound applied to the plate. It was found the frost formation process on the flat surface was considerably restrained due to the effect of ultrasound. Tan et al. (2015) developed a new method of defrosting using ultrasonic vibrations applied on the fins to avoid frost formation. The results of the experiments were a small frost layer formed and a COP improvement between 6.51% and 15.33%. Wang et al., (2012) reported that the frost growing on the evaporator was suppressed by using ultrasonic vibrations. They concluded that the basic ice layer on the fins will not be removed with ultrasonic vibrations, but frost crystals and frost branches on the ice layer were fractured and removed effectively. Li et al., (2014) found that the frozen water droplets adhered to cold vertical surface were instantaneously shed off due to the combined effects of the interface transverse shear force induced by the ultrasonic mechanical effect and the impact force generated by the ultrasonic acoustic pressure. They reported that the shedding process of frozen water droplets cannot be attributable to the heat effect generated by ultrasonic vibration, although the internal temperatures of the cold flat have an apparent rise due to the effect of ultrasonic vibration.

3.2.4 Radiation based defrost

Most of the existing electric heaters used for defrosting of heat exchangers use the infrared radiation and convective heat transfer to melt the frost layer from the surface. While this process has been deployed for several years, it is highly energy inefficient as pointed out in Section 3.1.2. There are rare studies for the utilization of radiation other than infrared for the defrost process. Kim (2012) conducted an experimental and modeling study to investigate the feasibility of using microwave radiation for the defrost process of a refrigerator. He found the position of the magnetron relative to an evaporator did not affect the uniformity of melting of the frost layer.

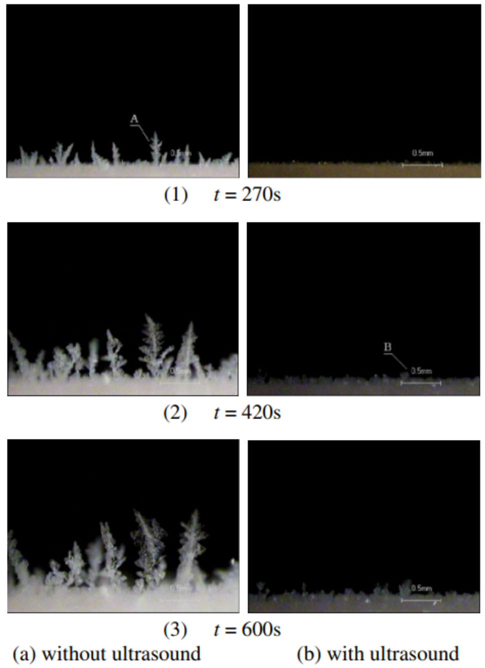

Fig. 14: Side view of frost formation comparison (50X magnification)

4. DEFROST CONTROL STRATEGIES

The use of demand defrost strategies has been investigated in several applications including domestic refrigerators, heat pumps and commercial refrigerated display cases. The techniques to initiate and terminate defrost cycles which have been studied include the following:

- Time-temperature controlled defrost
- Air pressure differential or air flow rate across the evaporator
- Temperature difference between the air and the evaporating surface
- Air-side and refrigerant-side heat transfer comparison
- Refrigerant flow rate measurement
- Fan power measurement
- Optical or acoustic measurement of ice thickness
- Artificial intelligence-based defrost control systems.

A discussion of several of these demand defrost techniques is given below.

4.1 TIME-TEMPERATURE CONTROLLED DEFROST

The most basic and commonly used defrost control strategy for supermarket applications is the timed defrost. The refrigerated display case evaporators are defrosted according to a predefined defrost schedule in which a timer both initiates and terminates the defrost cycle. Since this strategy is not based on the actual amount of frost present on the evaporator, it is possible that the defrost cycle is either insufficient in duration such that the frost is not completely removed during the defrost cycle or it is excessive in duration such that significantly more heating is supplied than that which is required to remove the frost.

The efficiency of the timed defrost strategy may be improved by using a temperature-controlled termination. In this technique, the defrost cycle is terminated when the evaporator temperature has reached a predetermined temperature, or when the defrost cycle has reached a predetermined duration, whichever occurs first. The temperature termination allows the defrost cycle to end earlier than that which would have occurred with only a timer. However, since the evaporator temperature is only used to terminate a defrost cycle, the possibility still exists that a defrost cycle will be initiated when none is required. While it is not energy efficient, the timed initiation/termination defrost control strategy is most often used in supermarket applications because it has the lowest first cost as well as being simple, robust and easy to maintain.

4.2 TIME-PRESSURE CONTROL

As an alternative to temperature-controlled termination, defrost may also be terminated based on pressure. In this technique, the defrost cycle is terminated when the evaporator pressure has reached a predetermined pressure deemed sufficient to melt all of the frost, or when the defrost cycle has reached a predetermined duration, whichever occurs first. The pressure termination allows the defrost cycle to end earlier than that which would have occurred with only a timer. However, since the evaporator pressure is only used to terminate a defrost cycle, the possibility still exists that a defrost cycle will be initiated when none is required.

4.3 TEMPERATURE MEASUREMENT

Borton and Walker (1993) discuss a demand defrost strategy that is based on the temperature difference between the display case discharge and return air. Their demand defrost controller measures the air curtain temperature at the outlet of the discharge and the inlet of the return to determine if defrost is needed. If the difference between these temperature measurements is greater than a predetermined set point for a sustained period of time, and a minimum amount of time has elapsed since the last defrost, then defrost is initiated. Furthermore, defrost is initiated if the elapsed time since the last defrost exceeds a specified maximum time between defrosts. The defrost cycle is terminated either on the basis of time or evaporator temperature (Borton and Walker 1991). The defrost controller was field tested in a supermarket with a sales area of 60,000 ft^2 (5,570 m^2), controlling the defrost of the low temperature display cases. Based on the results of the field testing at this supermarket, it was estimated that the demand defrost controller could reduce the annual energy consumption by 20,000 kWh for hot gas defrost systems and 62,000 kWh for electric defrost systems (including the energy savings of both the electric defrost heaters and the compressors).

Topper et al. (2001) describe a technique for demand defrost in which the air temperature within the refrigerated display case and the refrigerant temperature within the evaporator are measured. If the difference between the air temperature and the refrigerant temperature exceeds a predetermined threshold, then defrost is initiated. Since the rate of heat transfer between the air and the evaporator is reduced as ice builds up on the evaporator, the temperature of the air within the display case increases. Therefore, the temperature difference between the refrigerant and the air is indicative of frost formation on the evaporator. In the method described by Topper et al. (2001), a coefficient is used to modify the minimum temperature difference used to initiate defrost. For example, if doors are used on the display case, the time between defrost cycles may be extended if the frequency of door openings is low. Thus, the defrost threshold may be relaxed by modifying the value of the defrost coefficient. Topper et al. suggested that the defrost cycle should be terminated based on refrigerant temperature exceeding a predetermined value or the defrost time exceeding a predetermined value (typically 45 minutes). The performance of this demand defrost system was not reported.

Demand defrost strategies based on the measurement of evaporator air inlet and outlet temperatures require the use of simple, durable temperature sensors. Since at a minimum, only two sensors are required, it is expect that these sensors can be easily installed within a refrigerated display case. Maintenance of these sensors would be minimal, however, sensor replacement may be difficult.

4.4 AIR FLOW MEASUREMENT

Jarrett (1972) designed a fluid amplifier which can monitor the air pressure difference across the evaporator to detect the accumulation of frost on the evaporator and to initiate the defrost cycle. The fluid amplifier was tested in a domestic refrigerator, and it was shown that the device was capable of detecting the need for defrost based on the pressure difference across the evaporator. The original timed defrost controller installed in the domestic refrigerator initiated defrost every seven hours. With the fluid amplifier demand defrost controller, the interval between defrost cycles could be extended by three or four times that of the timed defrost interval when the door of the refrigerator or freezer was not opened and no loads were present within the refrigerator or freezer.

Hahn and Broyles (1968) utilized a technique in which the defrost cycle for a domestic refrigerator was initiated based on air-flow monitoring. Two separate and parallel air flow paths were created within the refrigerator: one air flow path contained the evaporator while the other air flow path (the reference channel) was clear of obstructions. The flow rate differential between these two flow paths was monitored by measuring the temperature of heated elements placed in each of the flow paths. As the air flow within the evaporator channel decreases due to frost formation, the temperature of the sensing element in the evaporator flow path increases. In addition, the air flow through the reference channel increases as the flow through the evaporator channel decreases. Thus, the temperature of the sensing element in the reference channel decreases. After a predetermined difference exists between the temperatures of the sensing elements, the defrost cycle is initiated. The defrost cycle is terminated when the temperature of the evaporator reaches a sufficiently high value to ensure that all the frost has been removed. Hahn and Broyles tested the demand defrost system in a domestic refrigerator both in the laboratory and in the field. They found that the system initiated defrost cycles as often as three times a day under high temperature and high humidity conditions, and as seldom as once in 15 days under low humidity and very low usage.

The measurement of airflow requires relatively complex airflow sensors which may not be sufficiently robust for application in refrigerated display cases. The long-term reliability and durability of airflow sensors is expected to be low.

4.5 HUMIDITY MEASUREMENT

Bell (1978) describes a humidity controlled technique used to initiate the defrost cycle for domestic refrigerator applications. A timing circuit was designed to vary the time between defrost cycles based upon the relative humidity in the refrigerated space. If the refrigerated space were maintained at 100% relative humidity, the time between defrosts was set to be 12 hours. As the relative humidity in the refrigerated space decreased, the time interval between defrosts increased. In experimental testing with a domestic refrigerator, it was found that the demand defrost system was capable of initiating defrost in 12 hours during severe usage and defrost could be delayed for several weeks under very light usage.

Fluctuations in domestic refrigerator humidity levels are expected to be low and the overall humidity level would be relatively uniform with time, since, in domestic refrigeration applications, the frequency of usage and door openings is relatively low compared to that of commercial refrigerated display cases. Thus, demand defrost methods based on humidity measurement may work well only in low-use domestic refrigeration applications. Furthermore, the slow response time and relatively low accuracy, particularly at high humidity levels, of inexpensive humidity sensors may not provide reliable control in the high humidity environment of refrigerated display cases. However, the current trend in better humidity control within supermarkets, particularly in the areas near the refrigerated display cases, may be sufficient to overcome the weaknesses of humidity-based demand defrost strategies.

4.6 REFRIGERANT FLOW RATE

Lawrence (2004) and Lawrence and Evans (2008) describe a demand defrost technique in which the control system detects the variation in refrigerant flow through an evaporator to determine if defrost is needed. As frost builds on an evaporator, the amount of heat which can be removed by the evaporator decreases. When the frost accumulation has finally become too great, the thermostatic expansion valve which controls the flow of refrigerant through the evaporator is unable to maintain a stable flow of refrigerant through the evaporator. The expansion valve opens and closes rapidly, or “hunts”, as it tries to maintain the proper superheat at the evaporator outlet. Lawrence and Evans developed an algorithm which determines the onset of this flow instability based on measuring the superheat at the exit of the evaporator. The algorithm developed by Lawrence and Evans was tested in a laboratory setting using an 8.2 ft (2.5 m) low temperature coffin case with electric defrost. It was found that, on average, the demand defrost algorithm initiated defrost every 38.8 hours, whereas the display case manufacturer suggested that the case be defrosted every eight hours. Therefore, it was estimated that the annual defrost energy use of the 8.2 ft (2.5 m) coffin case, using the demand defrost algorithm, would be 538 kWh versus 1960 kWh for the standard defrost every 8 hours. This results in an electrical defrost energy savings of 73%.

Estimation of the stability of refrigerant flow through an evaporator, based on the measurement of superheat at the evaporator outlet, requires the use of a simple, durable temperature sensor. However, the temperature data must be analyzed by a control module to determine the onset of flow instability. This control module will increase the initial cost of this demand defrost system and may require training for proper installation and operation.

4.7 COMPARISON OF AIR-SIDE AND REFRIGERANT-SIDE HEAT TRANSFER RATE

Thybo et al. (2002) were able to determine the onset of evaporator icing in refrigerated display cases using a technique which compared the air-side and the refrigerant-side heat transfer. By measuring the temperature and pressure of the refrigerant entering and exiting the evaporator, as well as the refrigerant flow rate, the refrigerant-side heat transfer can be calculated. In addition, by measuring the temperature of air entering and exiting the evaporator, and using air flow rate data provided by the display case manufacturer, the air-side heat transfer can be calculated. Thybo et al. (2002) suggest that by monitoring the residual, i.e., the difference between the measured air-side heat transfer and the refrigerant-side heat transfer, faults in the refrigeration system can be detected. When the residual is significantly different than zero, then a fault has occurred in the refrigeration system. This methodology was tested on a coffin-type display case in a laboratory setting and it was found that it was possible to determine the onset of a refrigeration system fault such as evaporator coil icing or a malfunctioning evaporator fan.

The technique proposed by Thybo et al. (2002) to determine the onset of refrigeration system faults by comparing the heat transfer on the refrigerant and air sides of the evaporator requires multiple temperature and pressure sensors, as well as mass flow sensors. The installation and maintenance of these sensors would be difficult. In addition, a control module would be required to process the data. Thus, the initial cost of this system would be high. Due to the complexity of the system, the long-term reliability of the system would be low.

Defrost strategies based on simpler air-side heat transfer measurements could be feasible in commercial refrigeration applications. In a simpler system, a heat flux sensor coupled with temperature sensors that measure air temperature and evaporator fin temperature could be used to determine the thermal resistance of the frost layer as it develops on the evaporator surface. A sufficiently high thermal resistance could then be used to initiate a defrost cycle. The required temperature and heat flux sensors would be inexpensive and could be incorporated into an easily-installable device which mounts on the evaporator.

4.8 THERMAL INSULATION EFFECT

Llewelyn (1984) briefly describes a demand defrost technique which is based on the thermal insulation effect of the frost layer. Two sensors are used in the system: one in intimate contact with the evaporator coil and one positioned in the outlet air stream from the evaporator. However, no information is provided on how the system operates or how well the system performs.

4.9 OPTICAL SENSORS

Paone and Rossi (1991) report on the use of fiber-optic sensors to determine ice thickness and to control the operation of the defrost cycle. Two types of fiber-optic sensors are discussed: reflection type sensors and transmission type sensors.

Reflection type sensors shine light on the ice surface and receive the reflected light from the ice surface. The intensity of the reflected light is proportional to the distance between the sensor and the ice surface. The output voltage of the sensor is proportional to the intensity of the reflected light, and thus, this voltage may be used to determine the distance between the sensor and ice surface, or the thickness of the ice. Reflection type sensors produce a continuous output between the minimum and maximum ice thickness. Reflection type sensors must be mounted perpendicular to the ice formation for proper operation.

Transmission type sensors consist of a separate light transmitting device and a light receiving device. The transmitter and receiver are mounted parallel to the evaporator surface and in line-of-sight of each other, at a certain distance above the evaporator surface. As ice grows, it eventually blocks the transmission of light from the transmitter to the receiver. The output voltage from the transmission type sensor is a step function indicating that the ice is either below or above the line-of-sight of the transducer and receiver.

Paone and Rossi (1991) noted that the output voltage of the reflection type sensor was strongly affected by the surface reflection coefficient of the ice surface. Since the ice surface may take on various textures depending on how the ice is formed, thereby leading to various surface reflection coefficients, uncertainties can exist in the measured ice thickness. On the other hand, the transmission type sensor generates an ON/OFF signal depending upon whether the ice has grown to a sufficient thickness to block the light traveling from the transmitter to the receiver. Thus, ice surface quality does not affect the output of a transmission type sensor.

During testing of a transmission type optical sensor in a domestic refrigeration application, Paone and Rossi (1991) noted that humidity condensed and ice formed on the lenses of the fiber-optic sensor heads. This could comprise the reliability of the sensor output. However, this problem was remedied by mounting a cylindrical duct on the fiber-optic head. The cylindrical duct reduced the convective motion near the sensor heads, allowing the humidity to diffuse along the length of the tube before it reached the sensor head. For the domestic refrigerator application, it was found that a duct of 4 mm in diameter and 30 mm in length was sufficient to eliminate ice formation on the sensor heads.

Paone and Rossi (1991) concluded that measuring ice thickness and controlling defrost cycles with a transmission type fiber-optic sensor was technically feasible in a domestic refrigeration application. However, the unit cost of the sensors, which was reported to be US$100 to US$150, would add substantially to the cost domestic refrigerators. Since the price of a typical domestic refrigerator can range from $400 to $800, an additional $100 to $150 for a transmission type fiber optic demand defrost sensor is economically unfeasible in that application. Furthermore, Paone and Rossi (1991) did not report on the long-term performance and reliability of the sensor in harsh environments such as that encountered in refrigerated display cases.

Byun et al. (2006) have investigated the use of photo-couplers to detect frost build-up on the evaporator coils of heat pumps. In their laboratory study, the evaporator coil was divided into nine zones and an infrared emitter and receiver were placed in the center of each of the nine zones, between the evaporator fins. Multiple photo-couplers were employed across the face of the evaporator to accurately detect the initiation and propagation of frost.

As compared to the standard timed defrost cycle, Byun et al. found that the photo-coupler defrost system increased the heating period of the heat pump by 7% to 9%. In addition, the defrosting period was reduced by 18% to 74% using the photo-coupler defrost system. While Byun et al. note that the photo-coupler defrost system was effective in laboratory studies, the system was not tested extensively in the field to determine its reliability.

Wang et al. (2010) describe the use of a micro-camera and image processing technology to determine the thickness of frost on a cold surface. The accuracy of the microscopic image system was reported to be 0.01 mm. The system was laboratory-based, and not optimized for field or commercial use.

Xiao et al. (2009) and Xiao et al. (2010) characterize the performance of a photoelectric device for determining frost layer thickness. It was found that the photoelectric device could accurately estimate frost height. A defrost control strategy was suggested, based on the use of photoelectric technology. While the system was effective in laboratory studies, the system was not tested extensively in the field to determine its reliability.

The Refrigeration and Thermal Test Center at Southern California Edison has tested an optical demand defrost technology in a medium temperature open vertical refrigerated display case (Mitchell 2005). The technology consists of a light emitting diode (LED) which transmits light through a fiber optic cable. The light output from the fiber optic cable is focused on a lens which reflects light back to the fiber optic cable. The lens is mounted near the fins of an evaporator so that frost accumulates on the lens, coincident with frost formation on the evaporator. The frost accumulation on the lens affects the amount of light which is reflected back to the fiber optic cable and when the intensity of the reflected light reaches a preset threshold, a defrost cycle can be initiated. During testing, it was noted that water droplet adhesion on the optical detector caused the optical demand defrost system to erratically initiate defrost cycles. In addition, at one point during testing, the defrost system failed to initiate defrost when the entire evaporator was frosted. Finally, the optical demand defrost system was unable to maintain the temperature within the refrigerated display case below acceptable levels. Thus, RTTC concluded that the optical demand defrost system was not reliable for supermarket refrigeration applications.

A commercially available optical frost sensor is available, shown in Fig. 15 (New Avionics Corporation 2011). It is claimed that this device is capable of detecting various types of moisture including ice, snow, frost and condensation based upon optical opacity and optical refraction via its 3 mm diameter optical probe. An optional heating element to de-ice the optical sensor is available. The optical sensor is placed between any two evaporator fins to determine when the evaporator has frosted. The device then generates a control signal which is used by the refrigeration system to initiate a defrost cycle.

Fig. 15: Commercially available optical sensor (New Avionics Corporation)

Optical sensors can accurately determine the quantity of frost accumulated on an evaporator in a specific location. However, multiple optical sensors would be required to accurately determine the accumulation of frost over the entire evaporator. The durability of the optical sensors is expected to be low in refrigerated display case applications. In addition, if multiple optical sensors are used, the complexity of the system would be high and the long-term reliability of the system would be low. As noted by the RTTC during testing of an optical demand defrost system, the failure of the system in a relatively clean laboratory environment casts doubt on the system's ability to perform in a "dirty" supermarket environment (Mitchell 2005). If manufacturers' were to overcome the reliability issues associated with optical demand defrost methods, it could be reasonably expected that optical sensors using LEDs, along with modern electronics, could be used to produce a low cost and commercially viable demand defrost system.

4.10 ARTIFICIAL INTELLIGENCE

Allard and Heinzen (1981) (1988) propose a demand defrost technique in which the time required to defrost the coil is monitored and the time periods between defrosting are adjusted accordingly. If the actual defrost time is shorter than a predetermined optimal time, then not enough frost was allowed to accumulate on the evaporator. Thus, the defrost controller increases the amount of time between successive defrost periods so that more frost will accumulate. On the other hand, if the actual defrost time is longer than the predetermined optimal time, too much frost accumulated on the evaporator. Thus, the defrost controller decreases the amount of time between successive defrost periods. The demand defrost controller was field tested in a domestic refrigerator and it was found that over an extended period of time, the controller had reduced the frequency of defrost by nearly a factor of four.

Working with Johnson Controls/Encore, EPRI developed a proprietary defrost control algorithm for refrigerated display cases that learns continuously from the current defrost behavior to schedule the next defrost (Hindmond and Henderson 1998). The method is sensorless and uses the computing power of the energy management system to perform the defrost scheduling calculations. Thus, new sensors are not required to be installed to use this system.

The demand defrost technology developed by Hindmond and Henderson was field-tested at two supermarkets. One supermarket, located in New Jersey, had a plan area of 33,000 ft^2 (3,070 m^2) and included 244 linear feet (74 m) of display cases and 863 ft^2 (80 m^2) of walk-in freezers serviced by a total of 123 kW of electric defrost. The remainder of the display cases and walk-ins at the New Jersey supermarket used off-cycle defrost. The other supermarket, located in Florida, had a plan area of 26,000 ft^2 (2,420 m^2) and included 236 linear feet (72 m) of display case and 1,705 ft^2 (158 m^2) of walk-ins serviced by hot gas defrost. The remainder of the display cases (160 ft or 49 m) and walk-ins (932 ft^2 or 87 m^2) at the Florida supermarket used off-cycle defrost.

At the New Jersey supermarket, the Hindmond and Henderson demand defrost controller was able to increase the time between defrosts from one day to three days. The electric defrost heater operation was reduced by 63% on average. It was estimated that if the demand defrost controller were installed on all the electric defrost cases in the supermarket, the total direct energy savings would be 25,000 kWh per year. By including the indirect savings associated with compressor energy use, the total savings was estimated to 38,000 kWh per year.

The results presented for the Florida supermarket were mixed. Hindmond and Henderson noted that a majority, but not all, refrigerated display case zones exhibited the expected behavior that defrost operation increases with increasing relative humidity. It was noted that perhaps the method of defrost termination, which was based on analog temperature sensors, was either not functioning properly or not optimally configured. Thus, additional testing of the demand defrost controller was planned to be performed at the Florida supermarket.

Datta and Tassou (2002) developed a demand defrost controller for refrigerated display cases based on artificial intelligence and inexpensive sensors such as temperature probes and a timer. Based on laboratory experiments performed on a medium temperature, multi-deck display case, Datta and Tassou found that the velocity of the air exiting the evaporator coil was the best indicator of frost accumulation on the coil. The velocity of the exiting air was found to decrease with increasing frost accumulation. In addition, Datta and Tassou found that the evaporator temperature as well as the entering and exiting air temperature at the evaporator decreased with increasing frost accumulation.

Datta and Tassou noted that robust velocity probes, such as hot-wire anemometers, are very expensive and thus are not feasible for use in demand defrost controllers for refrigerated display cases. Therefore, they proposed to use the ambient temperature and relative humidity, evaporator temperature, entering and exiting air temperature at the evaporator and the time between defrosts to as input to an artificial intelligence based demand defrost controller. While these quantities are not as good a predictor of frost accumulation as is the velocity of the air exiting the evaporator, the sensors for measuring these quantities are much less expensive.

Using a Multi-Layered Perceptron (MLP) artificial neural network model, a demand defrost controller was developed and tested in a laboratory setting. It was found that the demand defrost controller produced a defrost energy savings of 25% for ambient space conditions of 72°F (22°C) and 55% RH. In addition, defrost energy savings of 50% were achieved for ambient space conditions of 72°F (22°C) and 35% RH. For the medium temperature, multi-deck case studied, the number of defrost cycles per day was reduced from four at 72°F (22°C) and 65% RH to three at 72°F (22°C) and 45% RH, and to 2 at 72°F (22°C) and 35% RH. Furthermore, it was found that demand defrost had no adverse effect on product temperature as compared to timed defrost.

While the technique was successful in the laboratory, Datta and Tassou did not investigate the effectiveness of the demand defrost controller in a supermarket setting. They noted that other controllers, which are dependent on ambient space temperature and relative humidity, are being investigated for implementation in refrigerated display cases.

The success of an artificial intelligence based demand defrost strategy depends upon the complexity of the system. Rather complex artificial intelligence based demand defrost systems, such as that suggested by Datta and Tassou (2002), which require the use of several temperature and humidity sensors as well as a control module which analyzes the collected data, may not be commercially viable. The installation and maintenance of the numerous sensors would be difficult. In addition, the initial cost of the system would be high. Due to the complexity of the system, the long-term reliability of the system would be low. Refrigeration system installers and supermarket personnel may require training to properly install and operate this type of defrost system.

However, simpler artificial intelligence based defrost strategies which modify the time between cycles based on the duration of previous defrost cycles, such as that used by Hindmond and Henderson (1998), require only a control module which performs the required calculations and initiates and terminates defrost using a simple, durable temperature sensor. The temperature sensor and electronic controls for such a system are not inherently more complex than that required for simple time/temperature-termination defrost and they could conceivably be used to produce a low cost and commercial viable demand defrost system.

4.11 MISCELLANEOUS PROCESSES

For domestic refrigeration applications, Knoop et al. (1988) developed a methodology to estimate the time interval between defrosts based on the number and duration of refrigerator door openings. In this method, door openings and their duration are monitored. Then, a new time between defrosts is calculated based on the door opening duration times and the compressor run time. It was found that this technique could vary the defrost interval from 19 hours to 152 hours.

Bejan et al. (1994) derived theoretical equations to determine the optimal on/off sequence for operating a domestic refrigerator and its defrost system. These equations provide a means to theoretically determine the minimal power required by the refrigerator, while maintaining the prescribed temperature of the cold space and removing the frost build-up.

Verma et al. (2002) describe various design strategies which could be used to reduce the performance degradation due to frosting of display case evaporators. They show that the interval between defrosts could be dramatically increased by using variable speed evaporator fans to maintain constant airflow over the evaporator. In addition, fin staging was also shown to result in significant performance improvements, particularly at low air velocities and high inlet humidities where most of the frosting occurs near the front of the evaporator.

Liu et al. (2006) describe the use of an anti-frosting paint to effectively retard frost nucleation and decrease frost deposition rate on cold surfaces. For low air relative humidity, less than 60%, and cold surface temperature of 14°F (−10°C), the coated surface remained frost-free for over 3 hours while the uncoated surface was completely covered by a dense and thick layer of frost. While this technique does not eliminate frost formation, it does delay the formation of frost, thus potentially lengthening the duration between defrost cycles.

5. CONCLUSIONS

Frost growth on the heat exchanger surface can significantly alter the system performance. Various frost mitigation strategies have been reviewed and compared for the deployment of heat pump and commercial refrigeration systems. Once the frost has grown various techniques to defrost the heat exchanger surface has been elaborated and the methods have been compared. Along with frost mitigation and defrost processes, some practical procedures for defrost control are presented towards the end. The comprehensive overview of the literature provides a state-of-the-art technology for various procedures deployed to effectively handle the issue of frost growth on the heat exchanger surfaces.

REFERENCES

Abdel-Wahed R. M., Hifni M. A., Sherif S. A., Hot water defrosting of a horizontal flat plate cooling surface, International Journal of Refrigeration, Volume 6, Issue 3, May 1983, Pages 152-154

Allard J. , Heinzen R., Adaptive defrost. IEEE Transactions on Industry Applications 24, no. 1 (1988): 39-42.

Allard J. J., R.A. Heinzen, Defrosting System using Actual Defrosting Time as a Controlling Parameter. United States of America Patent 4,251,988. February 24, 1981.

and improvement of energy efficiency, Applied Energy 110 (2013) 9–16

Bansal P., Fothergill D., Fernandes R., Thermal analysis of the defrost cycle in a domestic freezer. Int J Refrig 2010; 33:589–99.

Bejan A., Vargas J. V. C., Lim. J. S., When to Defrost a Refrigerator, and When to Remove the Scale from the Heat Exchanger of a Power Plant. International Journal of Heat and Mass Transfer 37, no. 3 (1994): 523-532.

Bell C. A., Investigation of a Demand-Actuated Defrost System for Residential Refrigerators. Energy 3, no. 4 (1978): 479-483.

Bertsch S. S., Groll E. A., Two-stage air-source heat pump for residential heating and cooling applications in northern U.S. climates. Int J Refrig 2008; 31:1282–92.

Borton D. N., Walker D. H., Demand Defrost Controller for Refrigerated Display Cases. United States of America Patent 4,993,233. February 19, 1991.

Borton, D. N., Walker, D. H., Development of a Demand Defrost Controller. Energy Authority Report 93-14, New York, NY: New York State Energy Research and Development Authority, 1993.

Bullard C., Chandrasekharan R., Analysis of Design Tradeoffs for Display Case Evaporators. ORNL/TM-2004/157, Oak Ridge, TN: Oak Ridge National Laboratory, 2004.

Byun J. S., Jeon C. D., Jung J. H., Lee J., The application of photo-coupler for frost detecting in an air-source heat pump, International Journal of Refrigeration 29, no. 2 (2006): 191-198.

Cai L., Wang R. H., Hou P. X., Zhang X. S., Study on restraining frost growth at initial stage by hydrophobic coating and hygroscopic coating. Energy Buildings 2011; 43:1159–63.

Chen X., Ma R., Zhou H., Zhou X., Che L., Yao S., Wang Z., Activating the microscale edge effect in a hierarchical surface for frosting suppression and defrosting promotion. Sci Rep 2013; 3:2515.

Choi HJ, Kim BS, Kang D, Kim KC. Defrosting method adopting dual hot gas bypass for an air-to-air heat pump. Appl Energy 2011;88:4544–55.

Da Silva D. L., Hermes C. J., Melo C., Experimental study of frost accumulation on fan-supplied tube-fin evaporators. Appl Therm Eng 2011; 31:1013–20.

Da Silva D. L., Melo C., Hermes C. J. L., Effect of frost morphology on the thermal-hydraulic performance of fan-supplied tube-fin evaporators. Appl Therm Eng 2017; 111:1060–8.

Datta D., Tassou S., Implementation of a defrost on demand control strategy on a retail display cabinet, New Technologies in Commercial Refrigeration. Urbana, IL: International Institute of Refrigeration, 2002. 218-226.
Dong H., Zhao R. J., Yun L., Yi D. B., Effect of fin types of outdoor fan-supplied finnedtube heat exchanger on periodic frosting and defrosting performance of a residential air-source heat pump. Appl Therm Eng 2014;69:251–60.
Dong J., Deng S., Jiang Y., Xia L., Yao Y., An experimental study on defrosting heat supplies and energy consumptions during a reverse cycle defrost operation for an air source heat pump, Applied Thermal Engineering, Volume 37, May 2012, Pages 380-387
EHPA, "European Heat Pump Market and Statistics Report," EHPA, Brussel, 2015.
Fukiba K., Inoue S., Ohkubo H., Sato T., 2009. New defrosting method using jet impingement for precooled turbojet engines. J. Thermophys. Heat Transfer 23, 533–542.
Hahn T. W., Broyles, J. D., Electronic refrigeration defrost control - Report of performance, IEEE Transaction on Industry and General Applications 4, no. 1 (1968): 114-119.
Henderson H. I., Khattar, M., Measured Impacts of Supermarket Humidity Level on Defrost Performance and Refrigerating System Energy Use, ASHRAE Transaction 105, no. 1 (1999): 508-520.
Heo J., Jeong M. W., Kim Y., Effects of flash tank vapor injection on the heating performance of an inverter-driven heat pump for cold regions. Int J Refrig 2010; 33:848–55.
Hill Phoenix. 2011. http://www.hillphoenix.com (accessed December 2017).
Hindmond J., Henderson H., Refrigerated Display Case Demand Defrost Controller: Field Demonstration Results. TR-112121, Palo Alto, CA: Electric Power Research Institute, 1998.
Hoffenbecker N., Klein S. A., Reindl D. T., Hot gas defrost model development and validation, International Journal of Refrigeration 28, no. 4 (2005): 605-615.
Huang D., Zhao R. J., Liu Y., Yi D. B., Effect of fin types of outdoor fan-supplied finned-tube heat exchanger on periodic frosting and defrosting performance of a residential air-source heat pump, Applied Thermal Engineering 69 (2014) 251-260.
Hussmann, 2011. http://www.hussmann.com (accessed December 2017).
Jang J. Y., Bae H. H., Lee S. J., Ha M. Y., Continuous heating of an air-source heat pump during defrosting
Jarrett J. H., A New Demand Defrost Control for Domestic Forced Draft Refrigerator/Freezers and Freezers, IEEE Transactions on Industry Applications IA-8, no. 3 (1972): 356-364.
Jhee S., Lee K. S., Kim W. S., Effect of surface treatments on the frosting/defrosting behavior of a fin-tube heat exchanger. Int J Refrig 2002; 25:1047–53.
Jiang Y. Q., Fu H. Y., Yao Y., Yan L., Experimental study on concentration change of spray solution used for a novel non-frosting air source heat pump system. Energy Buildings 2014; 68: 707–12.
Kim J. W., Analytical and experimental examination of microwave defrosting method on commercial refrigerator evaporators, 2012, PhD Dissertation, University of Illinois at Urbana-Champaign
Knoop D. E., Tershak A. T., Thieneman M., An Adaptive Demand Defrost and Two-Zone Control and Monitor System for Refrigeration Products, IEEE Transactions on Industry Applications 24, no. 2 (1988): 337-342.
Kosar D., Dumitrescu O., Humidity Effects on Supermarket Refrigerated Case Energy Performance: A Database Review, ASHRAE Transactions 111, no. 1 (2005): 1051-1060.
Kragh J., Jørgen R., Svend S., Mechanical ventilation with heat recovery in cold climates. Proceedings of the seventh Nordic symposium on building physics in Nordic countries. Technical University of Denmark; 2005. p. 1–8.
Kwak K., Bai C., A study on the performance enhancement of heat pump using electric heater under the frosting condition pump under frosting condition. Appl Therm Eng 2010; 30: 539–43.
Lawrence J. M. W., Defrost Control Method and Apparatus. United States of America Patent 6,718,778. April 13, 2004.
Lawrence J. M. W., Evans, J. A., Refrigerant flow instability as a means to predict the need for defrosting the evaporator in a retail display freezer cabinet, International Journal of Refrigeration 31, no. 1 (2008): 107-112.

Lee M, Kim Y, Lee H, Kim Y. Air-side heat transfer characteristics of flat plate finned-tube HEs with large fin pitches under frosting conditions. Int J Heat Mass Tran 2010; 53:2655–61.
Li D., Chen Z., Shi M., Effect of ultrasound on frost formation on a cold flat surface in atmospheric air flow, Experimental Thermal and Fluid Science 34 (2010) 1247–1252.
Li L. T., Wang W., Sun Y. Y., Feng Y. C., Lu W. P., Zhu J. H., Ge Y. J., Investigation of defrosting water retention on the surface of evaporator impacting the performance of air source heat pump during periodic frosting-defrosting cycles. Appl Energy 2014; 135:98–107.
Li Y., Chen G., Tang L., Liu L., Analysis on performance of a novel frost-free air-source heat pump system. Build Environ 2011; 46:2051–9.
Liang C. H., Wang F., Lü Y., Wu C. X., Zhang X. S., Zhang Y. F., Experimental study of the effects of fin surface characteristics on defrosting behavior. Appl Therm Eng 2015; 75:86–92.
Liu L., Wang H. Y., Zhang X. H., Meng S., Ma C. F., An experimental study on minimizing frost deposition on a cold surface under natural convection conditions by use of a novel anti-frosting paint, Part I: Anti-frosting performance and comparison with the uncoated metallic surface. Int J Refrig 2006; 29:229–36.
Liu Z., Wang H., Zhang X., Meng S., Ma C., An experimental study on minimizing frost deposition on a cold surface under natural convection conditions by use of a novel anti-frosting paint. Part I. Anti-frosting performance and comparison with the uncoated metallic surface, International Journal of Refrigeration 29, no. 2 (2006): 229-236.
Llewelyn D. S., A significant advance in defrost control, International Journal of Refrigeration 7, no. 5 (1984): 334-335.
Ma G., Zhao H., Experimental study of a heat pump system with flash-tank coupled with scroll compressor. Energy Buildings 2008; 40:697–701.
Madani H., Heat pump systems: Market and Technological trend, Stockholm: KTH, Department of Energy Technoloy, 2015.
Mei V. C., Gao Z., Tomlinson J. J., Frost-less heat pump. ASHRAE Trans 2002; 108:452–9.
Melo C., Knabben F. T., Pereira P. V., An experimental study on defrost heaters applied to frost-free household refrigerators. Appl Therm Eng 2013; 51:239–45.
Mitchell S. Optical Demand Defrost. Final Report, Project ET04.10, Refrigeration Technology and Test Center (RTTC), Irwindale, CA: Southern California Edison, 2005.
Moallem E., Hong T., Cremaschi L., Fisher D. E. Experimental investigation of adverse effect of frost formation on microchannel evaporators, Part 1: Effect of fin geometry and environmental effects. Int J Refrig 2013;36: 1762–75.
New Avionics Corporation. Ice Meister Model 9734 Industrial Ice Detecting Sensor System.
Nguyen M., Hewitt N., Huang M., Performance evaluation of an air source heat pump using economized vapor injection compressor and flash tank coupled with capillary tubes. In: Proceedings of international congress of refrigeration, Beijing, China, ICR07-E2-1110; 2007.
Niederer D. H., Frosting and Defrosting Effects on Coil Heat Transfer, ASHRAE Transaction 82, no. 1 (1976): 467-473.
Nishimura T. “Heat pumps-status and trends” in Asia and the Pacific. Int J Refrig 2002;25(4):405–13.
Okoroafor E. U., Newborough M., Minimizing frost growth on cold surfaces exposed to humid air by means of crosslinked hydrophilic polymeric coatings. Appl Therm Eng 2000; 20:737–58.
Paone N., Rossi G., Fiber-optic ice sensors for refrigeration, Proceedings of SPIE - The International Society for Optical Engineering 1511 (1991): 129-139.
Park J. S., Kim D. R., Lee K. S., Frosting behaviors and thermal performance of louvered fins with unequal louver pitch. Int J Heat Mass Tran 2016; 95:499–505.
Qu M. L., Xia L., Deng S. M., Jiang Y. Q., A study of the reverse cycle defrosting performance on a multi-circuit outdoor coil unit in an ASHP-Part I: Experiments. Appl Energy 2012; 91:122–9.
Qu M. L., Xia L., Deng S. M., Jiang Y. Q., An experimental investigation on reverse-cycle defrosting performance for an air source heat pump using an electronic expansion valve. Appl Energy 2012; 97:327–33.

Rafati N. M., Fauchoux M., Besant R. W., Simonson C. J., A review of frosting in air-to-air energy exchangers. Renew Sust Energy Rev 2014; 30:538–54.
Rainwater J. H., Five Defrost Methods for Commercial Refrigeration, ASHRAE Journal 51, no. 3 (2009): 38-51.
Shang P. J., Effect of pre-start fans on defrosting characteristics of air source heat pump. Refrig Air Cond 2009;9(6):54–9.
Shao S., Wang B., Xia J., Ma G., Study on heat pump cycle for cold regions with twostage compression in one scroll compressor. In: 7th IEA heat pump conference, Beijing, China; 2002.
Sommers A. D., Jacobi A. M., Air-side heat transfer enhancement of a refrigerator evaporator using vortex generation. Int J Refrig 2005; 28:1006–17.
Sommers A. D., Truster N. L., Napora A. C., Riechman A. C., Caraballo E. J., Densification of frost on hydrophilic and hydrophobic substrates - examining the effect of surface wettability. Exp Therm Fluid Sci 2016; 75:25–34.
Song M. J., Chen A. L., An experimental study on defrosting performance of an ASHP unit with a multi-circuit outdoor coil at different frosting evenness values. Appl Therm Eng 2016a; 94:331–40.
Song M. J., Deng S. M., Pan D. M., Mao N.. An experimental study on the effects of downwards flowing of melted frost over a vertical multi-circuit outdoor coil in an air source heat pump on defrosting performance during reverse cycle defrosting. Appl Therm Eng 2014; 67:258–65.
Song M. J., Mao N., Deng S. M., Xia Y. D., Chen Y., An experimental study on defrosting performance for an air source heat pump unit at different frosting evenness values with melted frost locally drainage. Appl Therm Eng 2016c; 99:730–40.
Song M. J., Xia L., Mao N., Deng S. M., An experimental study on even frosting performance of an air source heat pump unit with a multi-circuit outdoor coil. Appl Energy 2016b; 164:36–44.
Sonobe N., Fukiba K., Sato S., Yoshimura Y., Method for defrosting heat exchangers using an air-particle jet. Int J Refrig 2015; 60:261–9.
Stoecker W. F., Industrial Refrigeration Handbook. New York: McGraw-Hill, 1998.
Su W., Zhang X. S. Performance analysis of a novel frost-free air-source heat pump with integrated membrane-based liquid desiccant dehumidification and humidification. Energy Buildings 2017; 145:293–303.
Tan H., Xu G., Tao T., Sun X., Yao W., Experimental investigation on the defrosting performance of a finned-tube evaporator using intermittent ultrasonic vibration, Applied Energy, vol. 158, pp. 220-232, 2015.
Tassou S. A., Datta D., Influence of Supermarket Environmental Parameters on the Frosting and Defrosting of Vertical Multideck Display Cabinets, ASHRAE Transactions 105, no. 1 (1999): 491-496.
Tassou S. A., Datta D., Marriott D., Frost formation and defrost control parameters for open multideck refrigerated food display cabinets, Proceedings of the Institution of Mechanical Engineers, Part A, Journal of Power and Energy 215 (2001): 213-222.
Thybo C., Rasmussen B. D., Izadi-Zamanabadi R., Detecting Air Circulation Faults in Refrigerated Display Cabinets." New Technologies in Commercial Refrigeration. Urbana, IL: International Institute of Refrigeration, 2002. 211-217.
Topper R., Gilliom R., Sanders J., Breland, J. Microprocessor Controlled Demand Defrost for a Cooled Enclosure. United States of America Patent 6,205,800. March 27, 2001.
Verma P., Bullard C. W., Hrnjak P. S., Design Strategies for Reducing Performance Degradation due to Frosting of Display Case Heat Exchangers, New Technologies in Commercial Refrigeration. Urbana, IL: International Institute of Refrigeration, 2002. 227-237.
Wang D., Tao T., Kang S., Xu. S., Non-contact frost thickness measurement by using a micro-camera and image processing technology, Proceedings of the 2010 IEEE, International Conference on Mechantronics and Automation. Xi'an, China: Institute of Electrical and Electronics Engineers, 2010. 288-293.
Wang D., Tao T., Xu G., Luo A., Kang S., Experimental study on frosting suppression for a finned-tube evaporator using ultrasonic vibration. Exp Therm Fluid Sci 2012; 36:1–11.

Wang F., Wang Z., Zheng Y. L. Z., Hao P., Huan, C. W. T., Performance investigation of a novel frost-free air-source heat pump water heater combined with energy storage and dehumidification, Applied Energy, vol. 139, pp. 212-219, 2015.
Wang Q, He W, Liu YQ, Liang GF, Li JR, Han XH, Chen GM. Vapor compression multifunctional heat pumps in China: a review of configurations and operational modes. Renew Sust Energy Rev 2012;16(9):6522–38.
Wang S. W., Liu Z. Y., Wang S. W., Liu Z. Y., A new method for preventing HP from frosting, Renewable Energy 30 (2005) 753–761
Wang W., Ma Z. L., Jiang Y. Q., Yao Y., Xu S., Yang Z., Field test investigation of a double-stage coupled heat pumps heating system for cold regions. Int J Refrig 2005;28(5):672–9.
Wang X., Hwang Y., Radermacher R., Two-stage heat pump with vapor-injected scroll compressor using R410A as a refrigerant. Int J Refrig 2009; 32:1442–51.
Wu X. M., Chu F. Q., Ma Q., Zhu B., Frost formation and frost meltwater drainage characteristics on aluminum surfaces with grooved structures. Appl Therm Eng 2017;118:448–54.
Wu X. M., Webb R. L., Investigation of the possibility of frost release from a cold surface. Exp Therm Fluid Sci 2001; 24:151–6.
Xiao J., Wang W., Guo Q. C., Zhao Y. H., An experimental study of the correlation for predicting frost height in applying the photoelectric technology, International Journal of Refrigeration 33, no. 5 (2010): 1006-1014.
Xiao J., Wang W., Zhao Y. H., Zhang F. R., An analysis of the feasibility and characteristics of photoelectric technique applied in defrost-control. International Journal of Refrigeration 32, no. 6 (2009): 1350-1357.
Yan Q. L., Zhu L., Zhang M. E., Yan N. X., Hui X. Y., Study on ultrasonic defrost technology of refrigeration fan. Trans Chinese Soc Agric Mach 2003; 34:74–85.
Yan W. M., Li H. Y., Tsay Y. L., Thermofluid characteristics of frosted finned-tube heat exchangers. Int J Heat Mass Tran 2005; 48:3073–80.
Yang D. K., Lee K. S., Song S., Fin spacing optimization of a fin-tube heat exchanger under frosting conditions. Int J Heat Mass Tran 2006; 49:2619–25.
Yang J., A study of heat pump fin staged evaporators under frosting conditions, 2003, PhD Dissertation.
Yao Y., Jiang Y. Q., Deng S. M., Ma Z. L., A study on the performance of the airside heat exchanger under frosting in an ASHP water heater/chiller unit. Int J Heat Mass Tran 2004; 47: 3745–56.
Ye H. Y., Lee K. S., Performance prediction of a fin-and-tube heat exchanger considering air-flow reduction due to the frost accumulation. Int J Heat Mass Tran 2013; 67:225–33.
Yin H. J., Yang Z., Chen A. Q., Zhang N., Experimental research on a novel cold storage defrost method based on air bypass circulation and electric heater. Energy 2012; 37:623–31.
Zhang P., Hrnjak P. S., Air-side performance evaluation of three types of heat exchangers in dry, wet and periodic frosting conditions, International Journal of Refrigeration, 32, 2009, 911-921
Zhang P., Hrnjak P. S., Air-side performance evaluation of three types of heat exchangers in dry, wet and periodic frosting conditions. Int J Refrig 2009; 32:911–21.
Zhnder M., Favrat D., Hohl H., Olivier C., Perevozchikov M., High performance airwater heat pump with extended application range for residential heating. In: 7th IEA heat pump conference, Beijing, China; 2002.
Zuo Z. P., Liao R. J., Zhao X. T., Song X. Y., Qiao Z. W., Guo C., Zhuang A. Y., Yuan Y., Antifrosting performance of superhydrophobic surface with ZnO nanorods. Appl Therm Eng 2017;,110:39–48.